Meteorologische Zeitschrift, Vol. **13**, No. 3, 209-219 (June 2004)

Article

Mapping of precipitation in Iceland using numerical simulations and statistical modeling

ÓLAFUR RÖGNVALDSSON[2,3], PHILIPPE CROCHET[1] and HARALDUR ÓLAFSSON[1,2,4*]

[1]Icelandic Meteorological Office, Reykjavík, Iceland
[2]Institute for Meteorological Research, Reykjavík, Iceland
[3]University of Bergen, Bergen, Norway
[4]University of Iceland, Reykjavík, Iceland

(Manuscript received August 8, 2003; in revised form January 8, 2004; accepted May 5, 2004)

Abstract

Precipitation in Iceland during a period of 10 years is simulated with the PSU/NCAR MM5 model. The results are compared with precipitation estimated by a statistical model based on observations and a number of topographic and geographic predictors. The simulated precipitation pattern agrees with the statistical model in areas where data is available and gives a credible precipitation pattern in data-sparse mountainous regions. The simulation is however in general overestimating the precipitation, but the magnitude and the seasonal and geographical distribution of the overestimation indicate that it is to some extent associated with observation errors that are due to wind-loss of solid precipitation. There are also uncertainties associated with the representativeness of the observations as well as with the reference model itself.

Zusammenfassung

Niederschlag in Island wurde mit dem PSU/NCAR MM5 Modell für eine 10-Jahresperiode simuliert. Die Modellresultate werden mit Niederschlagsschätzungen eines statistischen Modells verglichen, das auf Beobachtungen und auf einer Reihe von topographischen und geographischen Prediktoren basiert. Das simulierte Niederschlagsmuster stimmt für Gebiete, in denen Daten verfügbar sind, mit dem statistischen Modell überein und liefert in Gebirgsregionen mit schlechter Datenabdeckung glaubwürdige Niederschlagsmuster. Die Simulation ueberschätzt jedoch generell die Niederschlagsmengen. Dabei deuten die Amplitude und die saisonale und geographische Verteilung der Abweichung darauf hin, dass dies zu einem Teil mit Beobachtungsfehlern verknüpft ist, die durch windbedingte Verluste von festem Niederschlag entstehen. Zudem existieren Unsicherheiten in Zusammenhang mit der Repräsentativität der Beobachtungen sowie des Referenzmodells selbst.

1 Introduction

The aim of this study is to verify the precipitation simulated by a limited area atmospheric model, the PSU/NCAR MM5 (WANG et al., 2001), in Iceland. One of the reasons for using a limited area model to simulate precipitation is to obtain a dataset of the current climate for comparison with down-scaling of future climate from coupled atmospheric and oceanic simulations by GCMs.

Attempts have been made to simulate precipitation in mountainous terrain. In the recent PRUDENCE project simulations with five numerical models were compared to an observation-based reference in the Alps. The models performed quite satisfactorly, but produced consistently too little precipitation (FREI et al., 2003).

Precipitation in Iceland is largely associated with extra-tropical synoptic systems. It often occurs during strong winds and can be greatly enhanced locally by the mountainous terrain (DE VRIES and ÓLAFSSON, 2003). Due to this and a coarse observation network, the direct use of an interpolation method for mapping precipitation is considered not to be sufficiently reliable. To map the reference precipitation and to minimize the uncertainties related to scale issues (see TUSTISON et al. (2001)), some further modeling is therefore needed.

In the past years, various studies have described the statistical links between precipitation and topographic parameters (see for instance BENICHOU and BRETON (1987); DALY et al. (1994); BASIST et al. (1994); WOTLING et al. (2000); KIEFFER et al. (2001) and DROGUE et al. (2002)) and the joint effect of topographic and atmospheric parameters (KYRIAKIDIS et al., 2001). In the present paper, a similar approach is considered to model and map the precipitation of reference (hereafter called REF) used to verify the MM5 simulations.

This paper is organized as follows: In the next section we will give a short introduction to the observational data, followed by a short description of the models. The results will be presented in section 4, followed by discussions and concluding remarks. A more detailed

*Corresponding author: Haraldur Ólafsson, Bústaðavegur 9, IS-150 Reykjavík, Iceland, e-mail: haraldur@vedur.is

0941-2948/04/0013-0209 $ 4.95
DOI: 10.1127/0941-2948/2004/0013-0209

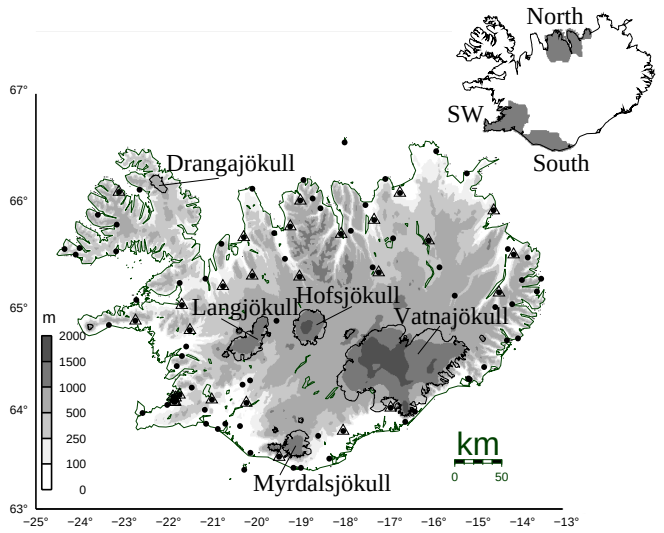

Figure 1: Map of Iceland showing regions North, South and SW (upper right corner) as well as position of rain gauges. Circles indicate the calibration network whilst triangles show the validation network. The largest glaciers are also shown.

Table 1: The geographic (top two) and topographic (bottom three) predictors used in SMOD.

	Geographic predictors:
1	D_{min} – minimum distance to the sea [km]
2	Y coordinates (lambert conformal) [km]
	Topographic predictors:
3	Smooth elevation [m]
4	Average slope steepness [%]
5	Average hillslope orientation, $-180^\circ < \theta < 180^\circ$ $0^\circ < \theta < 180^\circ$ clockwise from N to S $-180^\circ < \theta < 0^\circ$ clockwise from S to N

description of the mapping procedure is given in an appendix at the end of the paper.

2 Observational data

The observational precipitation data used in this study originates from 90 rain-gauges measuring daily precipitation (see Figure 1). The density of this network varies over Iceland. Most of the stations are located near the coast at elevations lower than 200 m, hence, data coverage is poor in the interior and in other high altitude regions. The measured precipitation may underestimate the true ground precipitation. The magnitude of the error depends on the wind-speed and the under-catch is more pronounced for solid (especially snow) than liquid precipitation (see review by HARALDSDÓTTIR et al. (2001), citing FØRLAND et al. (1996)).

In the present study, no correction was considered to account for the wind loss, or loss due to wetting or evaporation. This is mainly due to the fact that wind data is not available.

The season average monthly precipitation was derived over a ten year period from January 1991 to December 2000. The four seasons are defined as follows: March through May (MAM), June through August (JJA), September through November (SON) and finally December through February (DJF).

3 Model description

3.1 Statistical modeling

The statistical model (SMOD) used in this study makes use of five predictors. Two of them are related to the geographic position of the sites whilst the other three are related to the broad-scale topographic environment around the gauge sites (Table 1). The three topographic predictors were derived from a digital elevation model (DEM) of 1 km resolution (Figure 1), considering a 10 km averaging window. This choice was somehow arbitrary but in line with results suggested by other studies (see for instance DALY et al. (1994), and KYRIAKIDIS et al. (2001)). The slope steepness and orientation were defined with respect to a North (y) and East (x) plane. The statistical relationship between the season average monthly precipitation and the five predictors was evaluated individually for nine regions D and each season k by multivariate least-squares regression:

$$R(u,k) = a_{0,k,D} + \sum_{j=1}^{5} a_{j,k,D} p_{j,u} \quad (u \in D) \qquad (3.1)$$

where $R(u,k)$ is the season average monthly precipitation at location u and season k. Further, $p_{j,u}$ is the j^{th} predictor at location u and $a_{j,k,D}$ is the j^{th} regression coefficient for season k and region D. The nine regions were defined by merging together different topographic domains in order to have enough observations to calibrate the statistical model. These topographic domains were delineated by applying the method of the watershed transform (see for instance ROERDINK and MEIJSTER (2001)) to the reverted DEM, (DREM). In the DREM, the reverted elevation of each grid point rh_u, is defined by subtracting the DEM elevation h_u from the maximum DEM elevation h_{max}:

$$rh_u = h_{max} - h_u \qquad (3.2)$$

In doing so, the valleys become peaks and the peaks valleys, and the delineated "watersheds" defined the different massifs. Figure 2 presents the different regions. Table 2 gives the number of gauges and the approximate size of each region, of which some overlap. Table 3 summarizes the results of the multiple linear regressions. The predictors explain in average more than 80% of

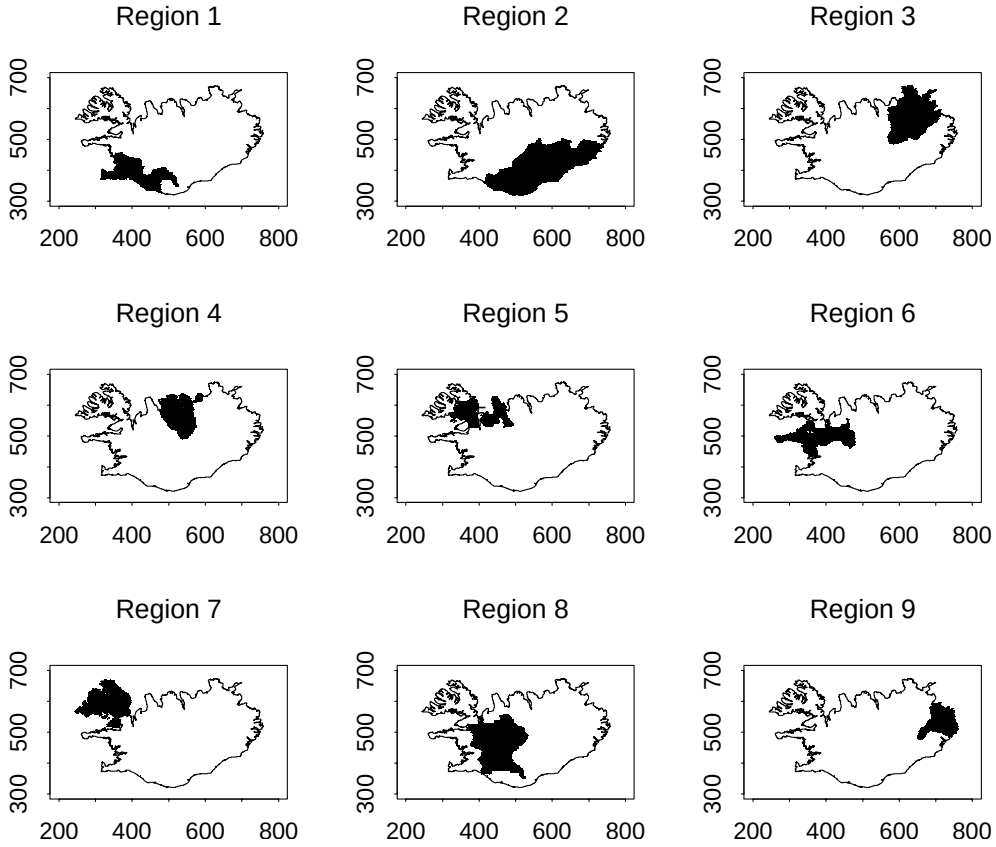

Figure 2: The nine different regions of SMOD (*D*). Scales are in km.

the variance of the season average monthly precipitation in Iceland for the considered period. The winter season (DJF) displays in average the poorest R-squared. This result suggests that the predictors are not as powerful to explain the complexity of the spatial variability of precipitation for this season with mixed precipitation phases and stronger wind regime as for the other seasons. Table 5, in the appendix, presents the regression equations. The poor network density makes the uncertainty of the regression coefficients relatively large. Nevertheless, it is worth noting that a positive relationship is observed between precipitation and elevation in most cases, with a more pronounced effect during SON and DJF than MAM and JJA. The exception is for region 3 at all seasons where higher precipitation amounts are observed by the coast than in the highlands, leading to a negative contribution of the elevation. The same negative contribution of elevation is observed during JJA for regions 7 and 9 where the network is mainly located in the bottom of steep narrow fjords or valleys. The relationship between precipitation and slope is negative in the north and northwest (regions 4, 5 and 7) at all seasons and positive elsewhere except in region 9 during DJF. This, together with the sign of the regression coefficient related to the orientation describe a precipitation enhancement and/or rain shadow effects along the hillslope according to its steepness and orientation. There is a negative relationship between precipitation and the latitude in the south and a positive relationship in the north. The contribution of the minimum distance to the sea is not clearly defined, but the tendency is a reduction of precipitation from the coast towards the inland, with some exceptions for regions where the available network is mainly coastal and where there is some correlation between elevation and distance to the sea.

A more comprehensive description of the precipitation mapping is given in the appendix.

Table 2: Region, number of gauges per region and the area of each region in km^2.

	MAM	*JJA*	*SON*	*DJF*
Region 1 (12276)	19	20	20	19
Region 2 (31060)	13	13	13	13
Region 3 (16628)	9	9	9	9
Region 4 (11208)	11	11	11	11
Region 5 (9528)	7	7	7	8
Region 6 (12492)	10	9	9	9
Region 7 (12816)	8	8	7	8
Region 8 (21272)	12	12	12	12
Region 9 (7636)	10	8	8	9

Table 3: Multiple R-squared and F ratio (in brackets). Bold characters show the lower R-squared value in each region.

	MAM	*JJA*	*SON*	*DJF*
Region 1	0.84 (13)	0.89 (22.5)	0.845 (15)	**0.7 (6)**
Region 2	0.65 (2.6)	0.75 (4.25)	0.61 (2.23)	**0.58 (1.9)**
Region 3	0.93 (8.2)	0.89 (5.2)	0.96 (13.4)	**0.87 (4.1)**
Region 4	0.76 (3.2)	**0.59 (1.5)**	0.73 (2.7)	0.72 (2.5)
Region 5	0.75 (0.6)	0.95 (3.7)	0.98 (9.8)	**0.55 (0.5)**
Region 6	0.92 (10.14)	**0.7 (1.4)**	0.9 (5.6)	0.89 (4.7)
Region 7	**0.83 (2)**	0.99 (59)	0.99 (818)	0.89 (3.4)
Region 8	0.89 (10.2)	**0.87 (8)**	0.88 (9.37)	0.9 (11.4)
Region 9	0.86 (5.1)	0.99 (74)	**0.83 (1.9)**	0.89 (5.2)
Mean R-squared	0.852	0.846	0.858	**0.777**

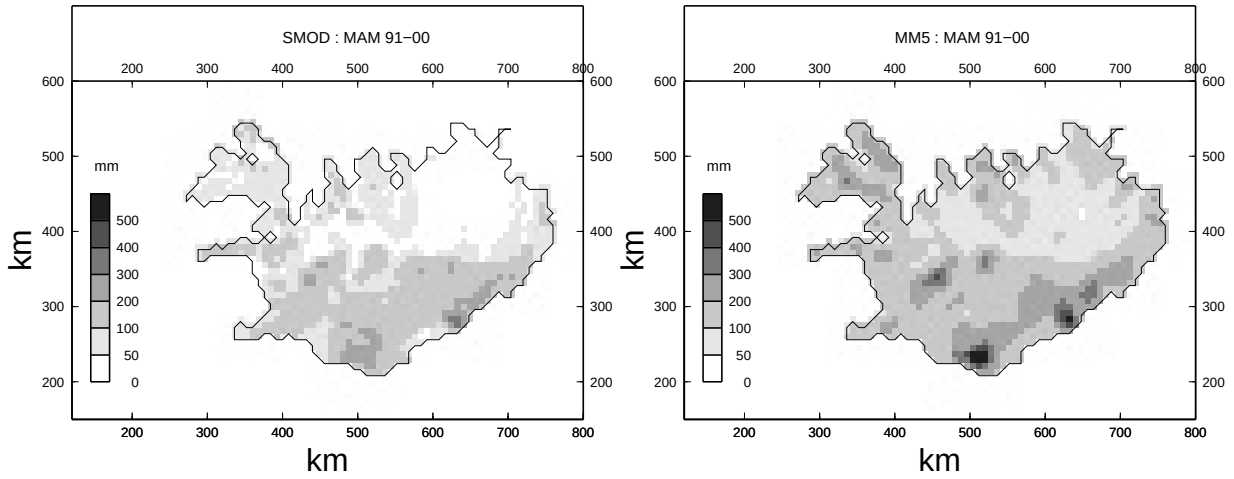

Figure 3: Season average monthly precipitation for MAM 1991–2000 [mm]. Reference precipitation is shown in (a) and simulated by MM5 in (b).

3.2 Numerical modeling

The PSU/NCAR MM5 model is a state of the art non-hydrostatic limited area model. It solves the pressure equations and the three dimensional momentum and thermo-dynamical equations that describe the atmosphere, using finite difference methods. The equations are integrated in time on an Arakawa-Lamb B grid using a second-order leapfrog scheme. Some terms, like the fast moving sound waves, are handled using a time-splitting scheme (DUDHIA, 1993). There is a terrain following vertical coordinate, σ, defined as:

$$\sigma = \frac{p_0 - p_t}{p_s - p_t}$$

Here p_0 is the reference pressure in a constant reference state, p_t is the constant pressure at the model top and p_s is the reference pressure at the surface.

3.2.1 Experimental setup

The domain used is 123 $\times$ 95 points, centered at 64° N and 19.5° W, with a horizontal grid spacing of 8 km. There are 23 vertical levels with the model top at 100 hPa.

In this study, the turbulent boundary layer is parameterized according to HONG and PAN (1996) and cloud physics and precipitation (microhpysics) processes according to GRELL et al. (1995) and REISNER et al. (1998), respectively. The version of the microphysical scheme used (Reisner2) includes cloud and rain water, as well as ice phase and super-cooled water. It further includes graupel and ice number concentration prediction equations. At the model top the radiation boundary condition formulated by KLEMP and DURRAN (1983) has been applied in order to minimize the reflection of vertically propagating gravity waves. Atmospheric long wave radiation is parameterized by the RRTM scheme, (MLAWER et al., 1997), and short wave radiation by DUDHIA (1993). For ground temperature we use the OSU/LSM scheme (CHEN and DUDHIA, 2001). The model, being run in a distributed memory mode, is forced by initial and boundary conditions from the European Centre for Medium range Weather Forecasts (ECMWF). The data used is from the ERA40 re-analysis project, having been interpolated from a horizontal grid of 1.25° to 0.5° prior to being applied to the MM5 modeling system.

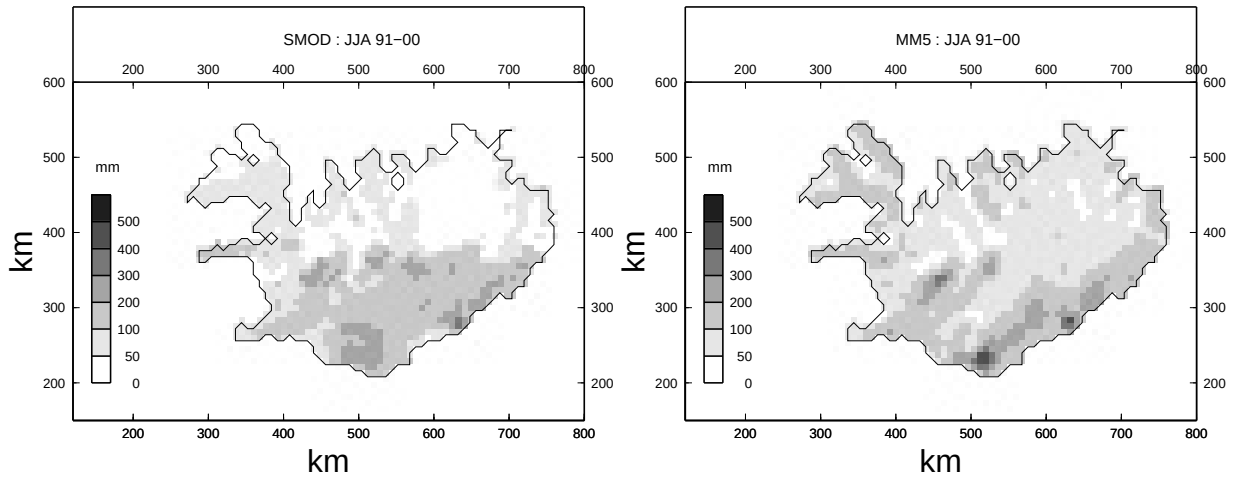

Figure 4: Season average monthly precipitation for JJA 1991-2000 [mm]. Reference precipitation is shown in (a) and simulated by MM5 in (b).

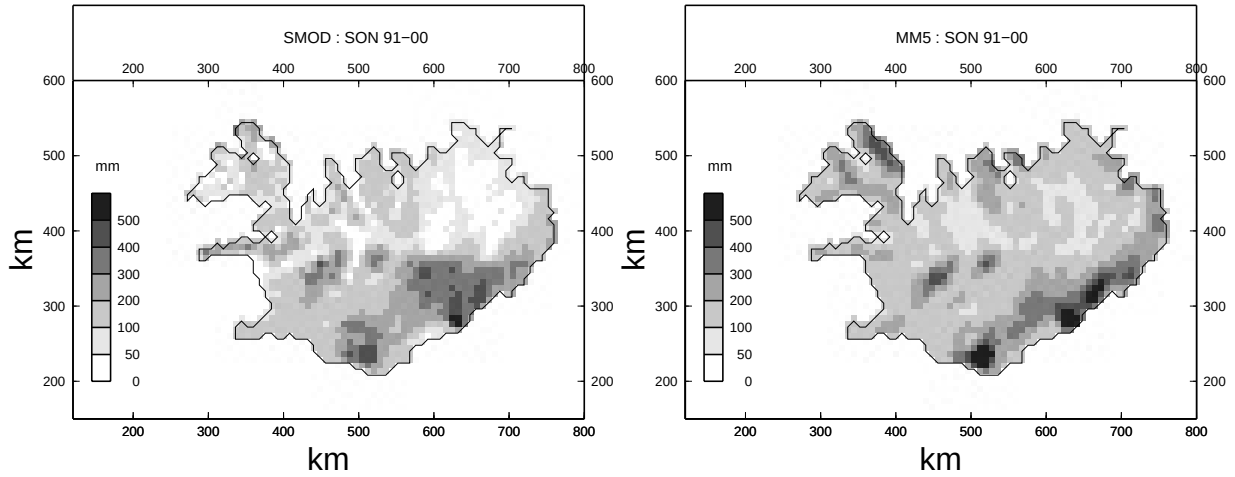

Figure 5: Season average monthly precipitation for SON 1991-2000 [mm]. Reference precipitation is shown in (a) and simulated by MM5 in (b).

4 Results

4.1 Qualitative comparison

The season average monthly precipitation for the period 1991 to 2000 is given in Figures 3 to 6. The overall pattern in the MM5 simulation is in a good agreement with REF, the greatest precipitation being along the south- and southeast-coast of Iceland. The precipitation gradient from southwest-Iceland to the northeast, towards Langjökull and Hofsjökull glaciers, is also present in both models. The precipitation gradients and the variability looks in general similar to REF, although being somewhat stronger in MM5. The most noticeable exceptions are in northwest-Iceland and at the northwest-part of Vatnajökull glacier. Estimation of precipitation in both these regions is uncertain, both due to lack of observations and the unrepresentative sampling of the topography of the regions by the observation network.

4.2 Quantitative validation

For quantitative validation of the numerical simulation, three regions have been defined. These regions are named North, South and SW and they are shown in the upper right corner of Figure 1. All these regions have a relatively dense observation network. In all regions, MM5 produces a precipitation pattern which agrees fairly well with the reference. Figure 7 shows the mean absolute relative error of precipitation simulated by MM5 compared to the reference precipitation. In the North the numerical simulation overestimates the observed precipitation from December to May by $110-130\%$, while the overestimation in summer and fall is around 80%. In the SW region the mean simulated precipitation is overestimated by about $20-50\%$ with the largest error being in the winter and spring. In the South the overestimation during summer and fall is about 30% and about 50% during spring and the winter months.

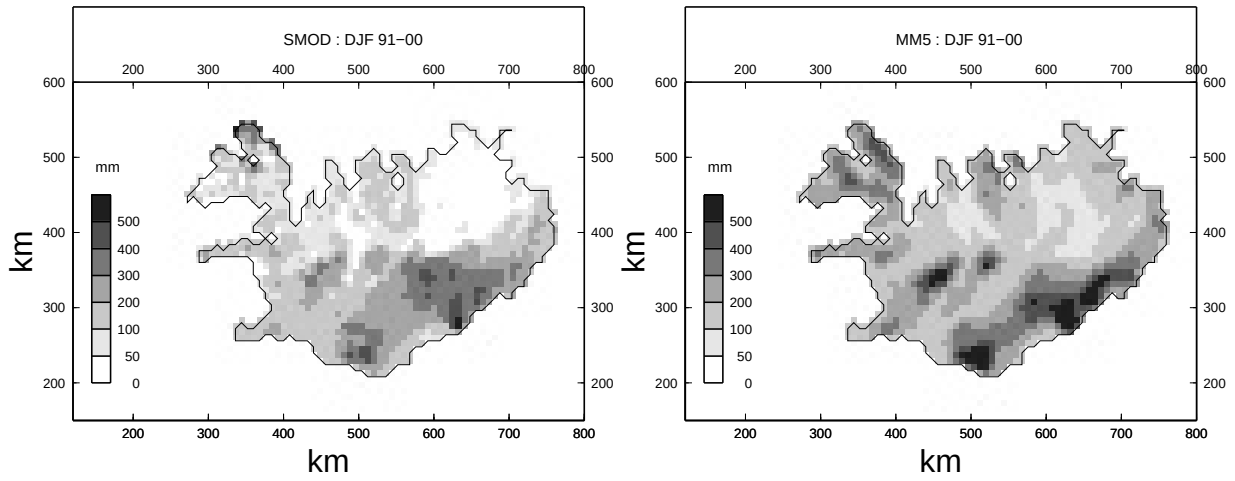

Figure 6: Season average monthly precipitation for DJF 1991-2000 [mm]. Reference precipitation is shown in (a) and simulated by MM5 in (b).

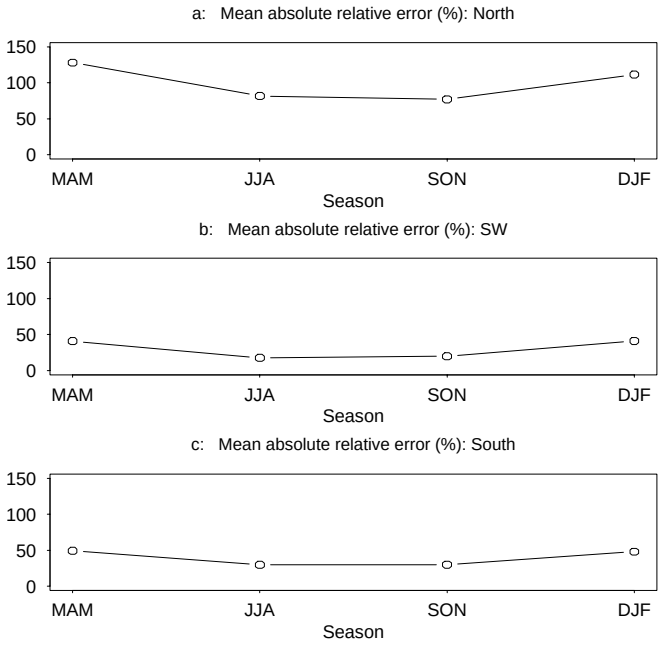

Figure 7: Mean absolute relative error [%], defined as $100 \cdot \frac{|MM5-REF|}{REF}$, of MM5 for regions (a) North, (b) SW and (c) South.

Figure 8 shows the precipitation as a function of altitude for all grid points in regions North and SW for both REF and MM5 during JJA. Figure 9 shows the same but for season DJF. It is clear that both the precipitation variability and the increase of precipitation with altitude (slope) is greater in MM5 than in REF in region North for both seasons. The slope is about four times that of REF in JJA and about double in DJF. It is also worth noting that the intercept, i.e. the precipitation at zero elevation, is higher in MM5 than REF, especially during the winter months. During these months the intercept in MM5 is about twice that of REF in region North. In JJA the intercept in MM5 is about 50% greater than in REF. In DJF the precipitation variability in regions SW and South (not shown) is similar to REF in MM5. The same holds true for JJA, but to a less extent. During the winter months the intercept is also slightly higher in MM5 and the slope being nearly twice the slope of REF. During JJA the intercept is nearly identical but the slope being again greater in MM5 than REF.

5 Discussion

The overestimation of precipitation in the MM5 simulations is greater in the north than it is in the south and southwest of Iceland. This is presumably due to both problems in the MM5 modeling system as well as greater uncertainties of the reference precipitation in the north. One source of uncertainty in the reference is the unrepresentativeness of the observation network. In fact, mapping of precipitation in complex terrain is highly depending upon the density of observations (e.g. FREI and SCHÄR (1998)). In Iceland, there is significant small scale variability in the orography and the observation sites are situated at low altitudes and close to the coast. This is particularly true for region North. The small scale variability in the orography introduces problems in the MM5 simulations as it is not resolved with the current resolution. Associated with this is that MM5 could be simulating to much precipitation at high altitudes, i.e. the precipitation gradient (slope) being to strong. The model could further be overestimating the background precipitation in the northern part of Iceland.

Another possible source of the discrepencies between REF and MM5 is that the reference is underestimating the true precipitation because of wind loss, wetting of the gauges and evaporation. This could explain to some extent the larger overestimation of MM5 during winter and spring than summer and fall. In strong winds conventional observations of solid precipitation

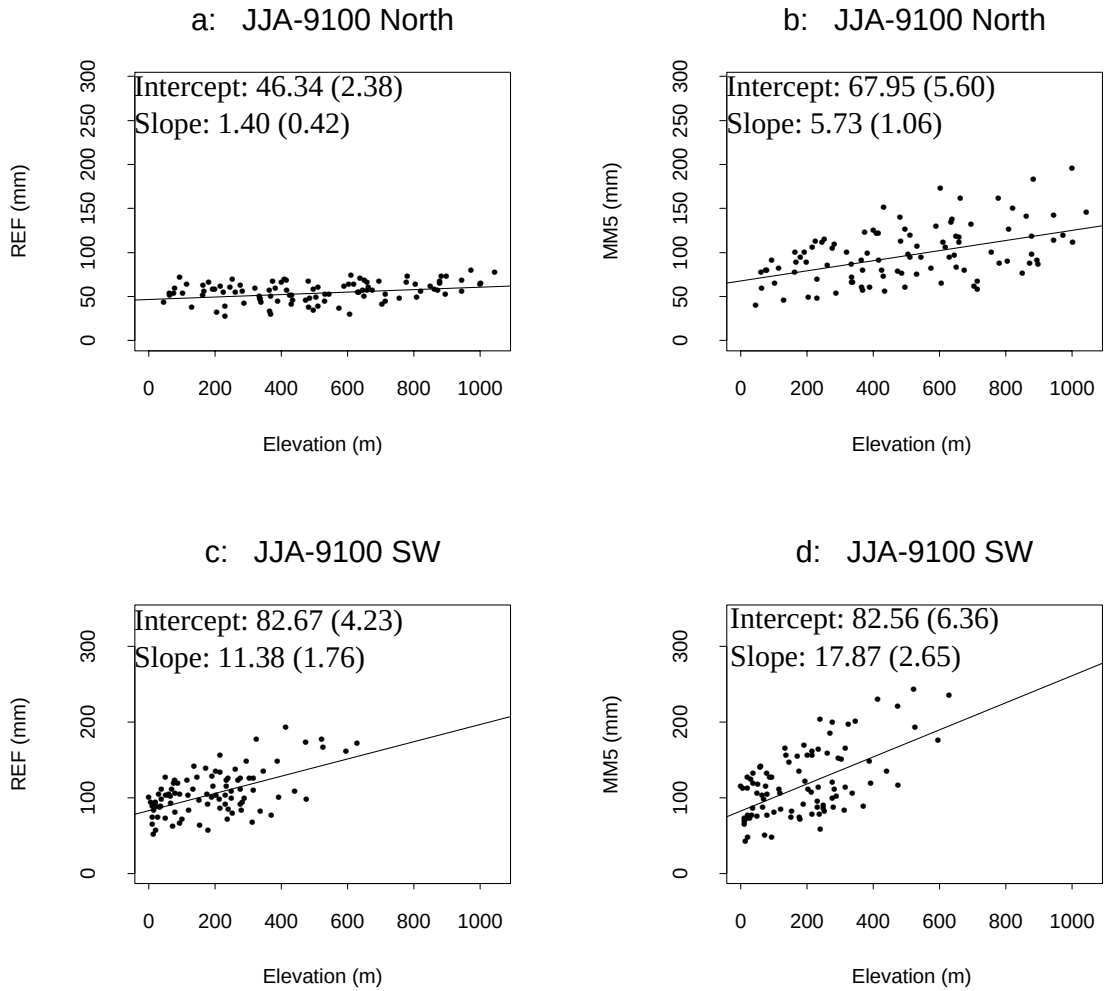

Figure 8: Season average precipitation as a function of elevation in JJA. (a) REF – region North, (b) MM5 – region North, (c) REF – region SW and (d) MM5 – region SW. Upper left corner of the figures shows the intercept [mm] and the slope [mm/100m]. Standard errors are shown in brackets.

underestimate grossly the true ground precipitation. Observation studies of solid precipitation (see review by HARALDSDÓTTIR et al. (2001)) suggest that at wind speeds greater than about 7 m/s, conventional precipitation gauges capture less than half of the true precipitation. Precipitation during winter and spring in region North (Figure 1) falls largely in the form of snow and often during strong winds. A large part of the overestimation of the simulated precipitation there may therefore be considered to be due to wind loss in the observations. If the precipitation is liquid, the wind loss is much less than if the precipitation is solid. This corresponds to the overestimation being less in the period June to November when most of the precipitation is liquid. In the summer and fall, there is still considerable overestimation of the precipitation in region North. The observed precipitation in the summer in the northern lowlands is typically only about 40 mm a month, but distributed over a relatively large number of days. In such weather, loss of observed precipitation due to wetting of the precipitation gauges and evaporation can also be expected to be of importance and observation errors therefore still account for some part of the difference between the two models.

In regions South and SW a much smaller part of the precipitation is solid, even during the winter. Accordingly, the simulation gives a much less overestimation than in the North. As in the North the greatest overestimation is in the winter and spring and loss of observed precipitation due to strong winds must still be regarded as an important source of error in the reference. The amount of precipitation in summer and fall is also considerably greater than in the North, and accordingly, loss due to wetting and evaporation is a smaller proportion of the total precipitation.

The results indicate that MM5 is overestimating the difference between upslope and downstream slopes as there is more precipitation variability for a given elevation than in REF. This may be related to the coarse resolution of the MM5 simulations.

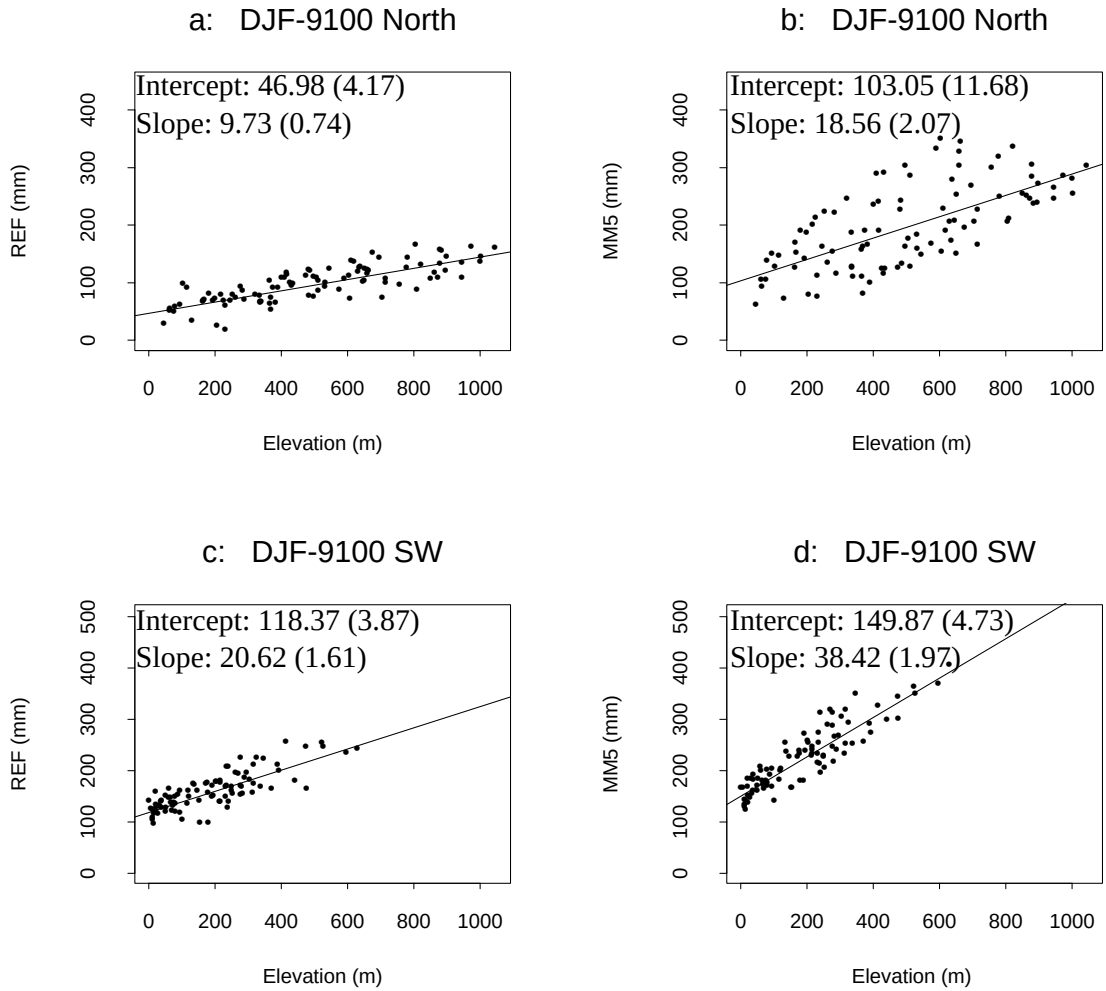

Figure 9: Season average precipitation as a function of elevation in DJF. (a) REF – region North, (b) MM5 – region North, (c) REF – region SW and (d) MM5 – region SW. Upper left corner of the figures shows the intercept [mm] and the slope [mm/100m]. Standard errors are shown in brackets.

Table 4: Cross validation – statistics of the estimation error for the 28 stations. Value found without using interpolation of residuals is shown in brackets.

	MAM	*JJA*	*SON*	*DJF*
MAE (%)	27.5 (27.7)	23.2 (23.9)	28.4 (28)	41.2 (40)
ME (mm)	3.38 (4.42)	2.5 (3.2)	7.7 (8.6)	4.6 (5.8)
STDEV (mm)	18.5 (18.8)	20.6 (20.6)	36.9 (36.4)	32.6 (32.1)

Simulations that were made over a number of subperiods revealed little sensitivity of the MM5 simulations to both the land surface scheme and the domain size for the domain used in the current simulations and a 45% larger domain.

As previously stated, almost all precipitation observation sites in Iceland are located below 200 m a.s.l. and REF must therefore be considered to be less reliable at high elevations than in the lowlands. The relatively high simulated values of precipitation in the mountains within the three regions may therefore be more realistic than a direct comparison with the current REF suggests.

6 Concluding remarks

A general conclusion is that the simulated precipitation agrees quite well with observed precipitation when taking into account errors in observations and modelling errors in REF. Considering the uncertainty of the reference in relation to both the precipitation loss and the modeling errors (MAE being about 30%, see Table 4), the MM5 simulations seem to reproduce the precipitation quite well in regions South and SW, but to much precipitation is simulated in the steep terrain in region North. The only obvious systematic errors in the simula-

Table 5: Regression coefficients for each season: (a) MAM, (b) JJA, (c) SON and (d) DJF. Standard error is shown in brackets.

MAM	*Intercept*	D_{min}	*Y*	*Elevation*	*Slope*	*Orientation*
Region 1	279 (77)	1.93 (0.64)	–0.55 (0.19)	0.024 (0.09)	7.21 (3.8)	–0.02 (0.08)
Region 2	413 (97)	0.52 (1.9)	–0.91 (0.28)	0.049 (0.36)	12.9 (12.2)	0.16 (0.13)
Region 3	–73 (87)	0.638 (0.62)	0.167 (0.13)	–0.09 (0.07)	5.36 (2.24)	0.09 (0.06)
Region 4	–196 (127)	–0.43 (0.71)	0.364 (0.2)	0.109 (0.06)	–0.69 (2.6)	–0.09 (0.09)
Region 5	149 (116)	0.24 (0.9)	–0.159 (0.2)	0.353 (0.32)	–14.8 (13)	–0.08 (0.16)
Region 6	177 (137)	–1.685 (1.6)	0.264 (0.26)	0.17 (0.21)	6.14 (3.9)	0.42 (0.14)
Region 7	–72 (325)	–25.3 (26)	0.49 (0.65)	0.218 (0.2)	–22.2 (12)	–0.20 (0.37)
Region 8	425 (54)	–0.39 (0.46)	–0.88 (0.14)	0.084 (0.06)	16.9 (5.8)	0.096 (0.08)
Region 9	33 (313)	–0.64 (1.24)	–0.003 (0.5)	0.01 (0.1)	4.83 (5.7)	0.36 (0.17)
JJA	*Intercept*	D_{min}	*Y*	*Elevation*	*Slope*	*Orientation*
Region 1	380 (74)	2.36 (0.6)	–0.83 (0.18)	0.015 (0.08)	7.6 (3.5)	–0.02 (0.08)
Region 2	404 (80)	1.37 (1.6)	–0.89 (0.23)	0.01 (0.29)	14.8 (10)	0.16 (0.11)
Region 3	110 (80)	–0.14 (0.57)	–0.98 (0.12)	–0.017 (0.06)	0.48 (2)	0.08 (0.56)
Region 4	–221 (135)	0.11 (0.77)	0.45 (0.21)	0.058 (0.07)	–2.28 (2.8)	–0.024 (0.1)
Region 5	78 (23)	0.2 (0.18)	–0.05 (0.04)	0.2 (0.06)	–8.4 (2.6)	–0,085 (0.03)
Region 6	68 (256)	–0.58 (3.13)	–0.065 (0.5)	0.05 (0.42)	7.6 (7.1)	0.18 (0.28)
Region 7	311 (57)	–1.13 (4.5)	–0.34 (0.11)	–0.05 (0.03)	–5.8 (2.25)	–0.003 (0.06)
Region 8	458 (64)	–0.64 (0.55)	–0.95 (0.16)	0.12 (0.08)	19 (6.9)	0.12 (0.1)
Region 9	–343 (50)	0.65 (0.29)	0.72 (0.08)	–0.14 (0.015)	6.9 (0.98)	0.34 (0.034)
SON	*Intercept*	D_{min}	*Y*	*Elevation*	*Slope*	*Orientation*
Region 1	441 (101)	2.18 (0.81)	–0.91 (0.25)	0.1 (0.1)	6.6 (4.8)	0.03 (0.11)
Region 2	465 (139)	–0.006 (2.7)	–0.97 (0.4)	0.19 (0.5)	15 (17)	0.24 (0.18)
Region 3	148 (128)	0.15 (0.9)	–0.13 (0.19)	–0.1 (0.1)	7.9 (3.3)	0.18 (0.09)
Region 4	–300 (251)	–1.4 (1.4)	0.62 (0.4)	0.21 (0.12)	–4.75 (5.2)	0.036 (0.18)
Region 5	88 (39)	0.08 (0.3)	–0.005 (0.06)	0.54 (0.1)	–23 (4.3)	–0.08 (0.05)
Region 6	–87 (230)	–5 (2.8)	0.26 (0.4)	0.6 (0.37)	5.2 (6.4)	0.7 (0.25)
Region 7	–695 (25)	–61 (1.5)	1.8 (0.05)	0.59 (0.01)	–50 (1.3)	–0.81 (0.02)
Region 8	603 (79)	–1.24 (0.7)	–1.26 (0.2)	0.2 (0.09)	24.9 (8.4)	0.16 (0.12)
Region 9	903 (1329)	–4.71 (6.2)	–1.36 (2.2)	–0.006 (0.25)	0.57 (19.8)	0.25 (0.579
DJF	*Intercept*	D_{min}	*Y*	*Elevation*	*Slope*	*Orientation*
Region 1	420 (140)	1.19 (1.16)	–0.8 (0.34)	0.16 (0.17)	5.4 (6.8)	0.08 (0.16)
Region 2	431 (127)	0.65 (2.5)	–0.86 (0.37)	0.17 (0.46)	12.5 (15.9)	0.17 (0.179)
Region 3	–48 (161)	0.53 (1.15)	0.14 (0.24)	–0.1 (0.13)	7.56 (4.1)	0.05 (0.11)
Region 4	–104 (237)	–1.46 (1.3)	0.22 (0.37)	0.19 (0.12)	–0.88 (4.9)	–0.13 (0.17)
Region 5	152 (174)	–1.01 (1.11)	–0.17 (0.29)	0.26 (0.34)	–6.9 (13.1)	0.0015 (0.2)
Region 6	346 (254)	–3.64 (3.1)	–0.54 (0.48)	0.4 (0.4)	0.65 (7)	0.65 (0.28)
Region 7	–1669 (553)	–92 (38)	3.9 (1.2)	1.04 (0.35)	–92 (31)	–1.28 (0.64)
Region 8	617 (74)	–1.11 (0.63)	–1.28 (0.19)	0.19 (0.09)	23.5 (7.9)	0.16 (0.11)
Region 9	953 (825)	–3.9 (2.6)	–1.5 (1.39)	0.21 (0.18)	–4.7 (13)	0.23 (0.31)

tions are most likely related to the horizontal resolution. At higher resolution more precipitation can be expected to be simulated at mountain peaks and less downstream of mountain ranges. Large differences between the two models in the mountains in the north underline the need for observations at high altitudes, both for the validation of the numerical simulations as well as for the development of SMOD and the precipitation mapping of Iceland. Due to strong winds and higher proportion of snow, estimation of precipitation by observations of snow accumulation may be a more feasible option than conventional rain-gauge observations.

Acknowledgements

The authors wish to thank Trausti JÓNSSON and Tómas JÓHANNESSON for discussions and for initiating the project. Comments from two anonymous reviewers further improved the article.

7 Appendix

7.1 Precipitation mapping

After the multiple linear regression equations are determined for each region D and each season k, the precipitation can be decomposed as the sum of two variables:

$$R(u,k) = SMOD(u,k) + e(u,k) \qquad (7.1)$$

where $SMOD(u,k)$ is the predicted precipitation from the statistical model and $e(u,k)$ is a random residual with zero mean and variance σ_e^2.

$$SMOD(u,k) = SMOD(u,k,D) = a_{0,k,D} + \sum_{j=1}^{5} a_{j,k,D} p_{j,u} \quad (u \in D) \qquad (7.2)$$

For the locations belonging to more than one region, the mean of the different predictions is taken:

$$SMOD(u,k) = E[SMOD(u,k,D)] \qquad (7.3)$$

The SMOD precipitation maps were produced for the following seasons: SON, DJF, MAM and JJA, by applying (7.2) and (7.3) to a regularly spaced grid of 2 km resolution. No spatial inconsistency was found in these maps after merging the different sectors together. Then, the residuals were interpolated using a spline function in tension (see SMITH and WESSEL (1990)) and added to the SMOD precipitation maps in order to produce to the final estimate, $\hat{R}(u,k)$:

$$\hat{R}(u,k) = SMOD(u,k) + \hat{e}(u,k) \qquad (7.4)$$

In order to assess the efficiency of the precipitation mapping, a cross-validation procedure was defined. A set of 28 validation stations located between 20 m and 400 m height were chosen (see Figure 1). One station was removed at the time, the statistical model re-calibrated each time and a new value estimated using (7.2), (7.3) and (7.4). Three statistical tests were then used to assess the mapping procedure.

The mean absolute error in %:

$$MAE\ [\%] = 100 \cdot E\left[\left|\frac{\hat{R}(u,k) - R(u,k)}{R(u,k)}\right|\right] \qquad (7.5)$$

The mean error:

$$ME = \left[\left(\hat{R}(u,k) - R(u,k)\right)\right] \qquad (7.6)$$

The standard deviation of the error:

$$STDEV = \sqrt{E\left[\left(\left(\hat{R}(u,k) - R(u,k)\right) - ME\right)^2\right]} \qquad (7.7)$$

The results (summarized in Table 4) show that according to MAE, the accuracy of the estimate is quite comparable for three seasons, and largest during DJF. These results are in agreement with the R-squared values of Table 3 and show the difficulty to model winter precipitation. The bias (ME) is always positive and largest during the wettest seasons (SON and DJF), and lowest for the driest seasons (MAM and JJA). The standard deviation of the error is also largest for the wettest seasons (SON and DJF) and lowest for the driest seasons (MAM and JJA).

7.2 Reference precipitation used to verify MM5

The horizontal resolution of MM5 is 8 km. A reference precipitation is defined for each MM5 grid point i and season k by taking the mean of all the point estimates (7.4) located within a 10 km circular window centered on that grid point:

$$REF(i,k) = E[\hat{R}(u,k)] \quad \| u - i \| \leq 5\text{km} \qquad (7.8)$$

7.3 Regression coefficients

Table 5 shows the regression coefficients for each season.

References

BASIST, A., G. D. BELL, V. MEENTEMEYER, 1994: Statistical Relationship between Topography and Precipitation Patterns. – J. Climate **7**(9), 1305–1315.

BENICHOU, P., O. L. BRETON, 1987: Prise en Compte de la Topographie pour la Cartographie des Champs Pluviométriques Statistiques. – La Météorologie **7(19)**, 23–24.

CHEN, F., J. DUDHIA, 2001: Coupling an Advanced Land-Surface/Hydrology Model with the Penn State/NCAR MM5 Modeling System. Part I: Model Implimentation and Sensitivity. – Mon. Wea. Rev. **129**, 569–585.

DALY, C., R. NELSON, D. PHILLIPS, 1994: A Statistical-Topographic Model for Mapping Climatological Precipitation over Mountainous Terrain. – J. Appl. Met. **33**, 140–158.

DROGUE, G., J. HUMBERT, J. DERAISME, N. MAHR, N. FRESLON, 2002: A Statistical-Topographic Model using an Omnidirectional Parametrization of the Relief for Mapping Orographical Rainfall. – Int. J. Climatol. **22**, 599–613.

DUDHIA, J., 1993: A Nonhydrostatic Version of the Penn State-NCAR Mesoscale Model: Validation Tests and Simulation of an Atlantic Cyclone and Cold Front. – Mon. Wea. Rev. **121**, 1493–1513.

FREI, C., J. H. CHRISTIANSEN, M. DÉQUÉ, D. JACOB, R. JONES, P. L. VIDALE, 2003: Daily precipitation statistics in regional climate models: Evaluation and intercomparison for the European Alps. – J. Geophys. Res. **108 (D3)**, ACL9–1–ACL9–19.

FREI, C., C. SCHÄR, 1998: A Precipitation Climatology of the Alps from High-Resolution Rain-Gauge Observations. – Int. J. Climatol. **18**, 873–900.

FØRLAND, E. P., P. ALLERUP, B. DAHLSTRÖM, E. ELOMA, T. JÓNSSON, H. MADSEN, J. PERÄLÄ, P. RISSANEN, H. VEDIN, F. VEJEN, 1996: Manual for operational correction of Nordic precipitation data. – Klima Report **24/96**, The Norwegian Meteorological Institute, Norway.

GRELL, G. A., J. DUDHIA, D. R. STAUFFER, 1995: A Description of the Fifth-Generation Penn State/NCAR Mesoscale Model (MM5). NCAR/TN-398+STR. National Center for Atmospheric Research, Boulder, CO, 107 pp.

HARALDSDÓTTIR, S. H., H. ÓLAFSSON, Y. DURAND, L. MÉRINDOL, G. GIRAUD, 2001: SAFRAN-Crocus snow simulations in an unstable and windy climate. – Annals of Glaciology **32**, 339–344.

HONG, S. Y., H. L. PAN, 1996: Nonlocal boundary layer vertical diffusion in a medium-range forecast model. – Mon. Wea. Rev. **124**, 2322–2339.

KIEFFER, A., WEISSE, P. BOIS, 2001: Topographic Effects on Statistical Characteristics of Heavy Rainfall and Mapping in the French Alps. – J. Appl. Met. **40**, 720–740.

KLEMP, J. B., D. R. DURRAN, 1983: An Upper Boundary Condition permitting Internal Gravity Wave Radiation in Numerical Mesoscale Models. – Mon. Wea. Rev. **111**, 430–444.

KYRIAKIDIS, P. C., K. JINWON, N. L. MILLER, 2001: Geostatistical Mapping of Precipitation from Gauge Data using Atmospheric and Terrain Characteristic. – J. Appl. Met. **40**, 1855–1877.

MLAWER, E. J., S. TAUBMAN, P. BROWN, M. IACONO, S. CLOUGH, 1997: Radiative Transfer for Inhomogeneous Atmosphere: RRTM, a Validated Correlated-K Model for the Longwave. – J. Geophys. Res. **102 (D14)**, 16663–16682.

REISNER, J., R. J. RASSMUSSEN, R. T. BRUINTJES, 1998: Explicit forecasting of supercooled liquid water in winter storms using the MM5 mesoscale model. – Quart. J. Roy. Meteor. Soc. **124B**, 1071–1107.

ROERDINK, J. B., A. MEIJSTER, 2001: The Watershed Transform: Definitions, Algorithms and Parallelization Strategies. – Fundamenta Informaticae **41**, 187–228.

SMITH, W. H. F., P. WESSEL, 1990: Gridding with continuous curvature splines in tension. – Geophysics **55**, 293 – 305.

TUSTISON, B., D. HARRIS, E. FOUFOULA-GEORGIOU, 2001: Scale issues in verification of precipitation forecasts. – J. Geophys. Res. **106 (D11)**, 11,775–11,784.

WANG, W., J. DUDHIA, D. GILL, Y. R. GUO, K. MANNING, J. CHISZAR, 2001: PSU/NCAR Mesoscale Modeling System Tutorial Class Notes and User Guide: MM5 Modeling System Version 3. www.mmm.ucar.edu/mm5/doc.html.

WOTLING, G., C. BOUVIER, J. DANLOUX, J. M. FRITSH, 2000: Regionalization of Extreme Precipitation Distribution using the Principal Components of the Topographical Environment. – J. Hydro. **233**, 86–101.